Heat Transfer Engineering

ISSN: 0145-7632 (Print) 1521-0537 (Online) Journal homepage: https://www.tandfonline.com/loi/uhte20

Numerical Investigation of Natural Convection in Heterogeneous Rectangular Enclosures

Silvio L. M. Junqueira , Fernando C. De Lai , Admilson T. Franco & José L. Lage

To cite this article: Silvio L. M. Junqueira , Fernando C. De Lai , Admilson T. Franco & José L. Lage (2013) Numerical Investigation of Natural Convection in Heterogeneous Rectangular Enclosures, Heat Transfer Engineering, 34:5-6, 460-469, DOI: 10.1080/01457632.2012.722437

To link to this article: https://doi.org/10.1080/01457632.2012.722437

Accepted author version posted online: 04 Sep 2012.
Published online: 04 Sep 2012.

Heat Transfer Engineering, 34(5–6):460–469, 2013

ISSN: 0145-7632 print / 1521-0537 online
DOI: 10.1080/01457632.2012.722437

Taylor & Francis
Taylor & Francis Group

Numerical Investigation of Natural Convection in Heterogeneous Rectangular Enclosures

SILVIO L. M. JUNQUEIRA,[1] FERNANDO C. DE LAI,[1] ADMILSON T. FRANCO,[1] and JOSÉ L. LAGE[2]

[1]Thermal Sciences Laboratory, Federal University of Technology-Parana, Curitiba, Brazil
[2]Mechanical Engineering Department, Southern Methodist University, Dallas, Texas, USA

The aim of this study is to investigate numerically the steady natural convection resulting from horizontally heating a rectangular enclosure filled with a fluid and containing uniformly distributed, conducting, fixed and disconnected solid blocks (i.e., not touching each other). In particular, the effects of solid volume fraction, solid–fluid thermal conductivity ratio, and total number of blocks on the heat transfer process are determined by solving the mass, momentum, and energy conservation equations using the finite-volume method. The enclosure aspect ratio is varied from 0.25 to 4, the Rayleigh number from 10^5 to 10^8, and the Prandtl number is set as unity. Results of the numerical simulations are presented in terms of the surface-averaged Nusselt number, streamfunction, and streamline and isotherm distributions. The interference phenomenon caused by the solid blocks on the natural convection process is considered in detail and used to explain and predict the surprising and complex behavior of surface-averaged Nusselt number.

INTRODUCTION

Natural convection is ubiquitous in geological formations. The oil industry, in particular, has interest in the natural convection of fluids within geological formations, as this process can affect the fluid percolation and by consequence the well drilling and production processes. The fluid percolation, associated with the adverse environment inside the well bore, for instance, can lead to the invasion of the drilling fluid toward fractures in the geological structure, which can eventually compromise the drilling process.

The geometric complexity of the heterogeneous domain found underground hinders the analysis of various parameters affecting the transport process. Modeling equations [1–3] can be developed using either the continuum approach or the porous-continuum approach [4]. For models with regular geometry, the former is preferable for being more precise than the latter, as each constituent of the system (fluid and solid) is considered separately.

A geometrically simple geological formation is a network of connected fractures saturated with a fluid, with the fractures modeled as regular paths formed by impermeable, disconnected, and conductive solid blocks distributed inside the domain. A related geometry was considered by House et al. [5] in the investigation of thermal conductivity effects on the natural convection in an enclosure containing a centered, single solid block. This study was extended by Oh et al. [6], Lee and Ha [7, 8], Zhao et al. [9], Zhao et al. [10], Bhave et al. [11], and Kumar De and Dalal [12]. A step toward more complex geometries was taken by reducing the size and increasing the number of blocks inside the enclosure, as in Merrikh and Mohamad [13], Merrikh and Lage [14, 15], Hooman and Merrikh [16], Braga and de Lemos [17] and Pourshaghaghy et al. [18]. All these studies were performed using the continuum approach. Comparison between continuum and porous-continuum approaches was done by Merrikh and Lage [14], Massarotti et al. [19], and Braga and de Lemos [20].

The effects of varying the solid-to-fluid thermal conductivity ratio (K), the fluid volume fraction (the porosity, ϕ), and the number of blocks (N) have never been investigated. Knowledge of these effects is fundamental in determining the heat transfer

The authors are thankful for the support provided by the TEP/CENPES/PETROBRAS, the Brazilian Petroleum Agency (ANP), the Human Resources Program for the Petroleum and Gas Sector PRH-ANP (PRH10–UTFPR), and the UTFPR Science Foundation (FUNTEF–PR).

Address correspondence to Professor José L. Lage, Mechanical Engineering Department, Southern Methodist University, 6425 Boaz Lane, Dallas, TX 75275-0337, USA. E-mail: jll@smu.edu

efficiency across the enclosure. This study presents numerical simulation results obtained through the solution of the continuum transport equations characterizing these effects for various enclosure aspect ratios (A) and Rayleigh numbers (Ra).

CONTINUUM MODEL: EQUATIONS AND BOUNDARY CONDITIONS

Figure 1 presents a schematic of the configuration considered here, including geometric parameters and boundary conditions, in nondimensional form, necessary for solving the transport balance equations. Noteworthy is the isothermal conditions imposed at the vertical surfaces of the enclosure (horizontal heating) and the adiabatic horizontal surfaces. The solid blocks are thermally active, inasmuch as they allow heat to diffuse through them, requiring that energy and momentum compatibility conditions be set along the solid–fluid interfaces.

The enclosure aspect ratio is $A = L/H$, with L being the width and H the height of the enclosure; U and V are the nondimensional velocity components in the X and Y directions, respectively. The left wall of the enclosure is kept at θ_H, and the right at $\theta_C < \theta_H$, with the gravity acceleration g acting downward in the vertical direction. Nonslip and impermeable velocity conditions are imposed along all solid surfaces in contact with the fluid.

The internal geometry of the domain is known to affect the natural convection process; hence, it has to be carefully described. The blocks are all square and distributed uniformly within the enclosure. The volume fraction of solid ϕ_s is related to the total number of blocks N_{tot} and the nondimensional side-length of the blocks D. For being more common in studies of flow in porous media, the complementary fluid volume fraction ϕ of the domain (known as porosity) is used here, where $\phi = V_f/V_T$, with V_f and V_T being the fluid total volume and the enclosure total volume, respectively.

The process is assumed to be steady. The fluid, filling completely (saturating) the enclosure voids, is assumed to be incompressible, single phase, and Newtonian. The solid and fluid constituents are considered homogeneous and isotropic, having constant and uniform properties. Viscous dissipation is considered negligible, and the buoyancy effect is modeled by the Oberbeck–Boussinesq approximation [1]. The fluid and solid constituents are treated individually, each with specific conservation equations that are linked via compatibility conditions at the solid–fluid boundaries. Hence, the nondimensional mass, momentum, and energy balance equations for the fluid are, respectively:

$$\frac{\partial U}{\partial X} + \frac{\partial V}{\partial Y} = 0 \tag{1}$$

$$U\frac{\partial U}{\partial X} + V\frac{\partial U}{\partial Y} = -\frac{\partial P}{\partial X} + Pr\left(\frac{\partial^2 U}{\partial X^2} + \frac{\partial^2 U}{\partial Y^2}\right) \tag{2}$$

$$U\frac{\partial V}{\partial X} + V\frac{\partial V}{\partial Y} = -\frac{\partial P}{\partial Y} + Pr\left(\frac{\partial^2 V}{\partial X^2} + \frac{\partial^2 V}{\partial Y^2}\right) + Ra\,Pr\,\theta \tag{3}$$

$$U\frac{\partial \theta}{\partial X} + V\frac{\partial \theta}{\partial Y} = \frac{\partial^2 \theta}{\partial X^2} + \frac{\partial^2 \theta}{\partial Y^2} \tag{4}$$

and the energy equation for the solid (blocks) is

$$0 = \left(\frac{\partial^2 \theta}{\partial X^2} + \frac{\partial^2 \theta}{\partial Y^2}\right) \tag{5}$$

where the nondimensional Cartesian coordinates, velocity components, pressure, and temperature are defined as:

$$(X, Y) = \frac{(x, y)}{H}; \quad (U, V) = \frac{(u, v)\,H}{\alpha_f};$$

$$P = \frac{p\,H^2}{\rho_f\,\alpha_f^2}; \qquad \theta = \frac{T - T_C}{T_H - T_C} \tag{6}$$

The Prandtl number, Pr, the Rayleigh number, Ra, and the solid–fluid thermal conductivity ratio, K, are nondimensional groups ruling the model, defined as:

$$Pr = \frac{\nu_f}{\alpha_f}; \quad Ra = \frac{g\beta H^3 (T_H - T_C)}{\nu_f \alpha_f}; \quad K = \frac{k_s}{k_f} \tag{7}$$

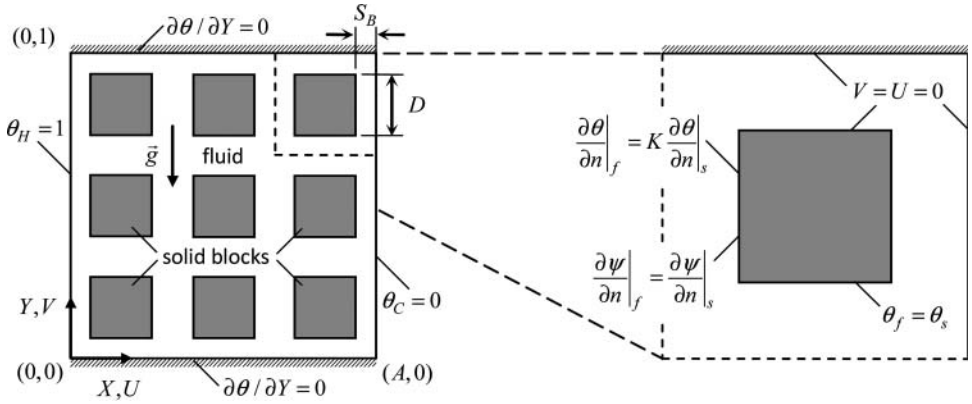

Figure 1 Heterogeneous medium made of uniformly distributed solid blocks (the inset details a single block) showing imposed boundary and compatibility conditions.

Observe that K affects the compatibility thermal condition imposed along the solid block surfaces (Figure 1). In the previous equations, (x,y) are the horizontal and vertical coordinates, (u,v) the velocity components, p the pressure, T_H and T_C the enclosure hot (left) and cold (right) wall temperatures, α_f the fluid thermal diffusivity ($\alpha = k/\rho c$, with c being the specific heat and k the thermal conductivity of the fluid or solid, indicated by the subscripts f or s, respectively), ρ_f the fluid density, ν_f the kinematic viscosity, and β the fluid isobaric coefficient of volumetric thermal expansion.

The dimensionless boundary conditions are:

$$U = V = 0 \quad \text{and} \quad \theta = 1 \quad \text{for} \quad X = 0;$$

$$U = V = 0 \quad \text{and} \quad \theta = 1 \quad \text{for} \quad X = 1 \tag{8}$$

$$\frac{\partial \theta}{\partial Y} = U = V = 0 \quad \text{for} \quad Y = 0 \quad \text{and} \quad Y = 1 \tag{9}$$

and the compatibility conditions at the solid–fluid interface along the solid block boundaries are:

$$U = V = 0; \quad \theta|_f = \theta|_s; \quad \left.\frac{\partial \theta}{\partial n}\right|_f = K \left.\frac{\partial \theta}{\partial n}\right|_s; \quad \left.\frac{\partial \psi}{\partial n}\right|_f = \left.\frac{\partial \psi}{\partial n}\right|_s, \tag{10}$$

where n is the unit vector perpendicular to the block boundary and Ψ is the nondimensional streamfunction (at each (i,j) node of the discretized numerical domain), defined as:

$$\psi = \psi_{i,j} = \psi_{i,j-1} + \int_{Y_{j-1}}^{Y_j} U_{i,j} dY = \psi_{i-1,j} + \int_{X_{i-1}}^{X_i} -V_{i,j} dX \tag{11}$$

satisfying Eq. (2) [21]. Observe that the combination of Eq. (11) and the boundary conditions Eqs. (8)–(10) yields the value $\Psi = 0$ along every solid boundary of the domain. Moreover, in Eq. (10), the interface compatibility conditions in speed and in streamfunction are in fact internal boundary conditions (nonslip and impermeable, respectively) for the fluid, while the temperature and temperature-derivative compatibility conditions enforce continuity of temperature and heat flow across the fluid–solid interface.

Solution of Eqs. (1)–(5) is obtained by means of the control volume method using the SIMPLEST algorithm [22]. The hybrid scheme is applied to interpolate the convective terms. Convergence is achieved whenever the sum of the absolute values of the local residue of each variable (U, V, P, θ), between two consecutive iterations, is less than 10^{-6}.

The surface-averaged Nusselt number is determined from the equation

$$Nu_{av} = \frac{h_{av} H}{k_f} = -\int_0^1 \left.\frac{\partial \theta}{\partial X}\right|_{X=0} dY \tag{12}$$

where h_{av} is the surface-averaged heat transfer coefficient. Notice that although at the steady state the surface-averaged Nusselt number becomes independent of the X location chosen for calculating it, the choice of $X = 0$ (as well as $X = 1$) simplifies the calculation because of the nonslip condition (no convection) along these two solid walls of the domain.

RESULTS AND DISCUSSION

Table 1 presents the ranges chosen for all the parameters, assuming Pr fixed and equal to unity. Observe that the total number of blocks in each enclosure N_{tot} is indicated by the group $N \times g_B$, where N represents the number of blocks used in a square lattice and g_B the number of lattices used to fill the enclosure, with $g_B = A$ when $A \geq 1$ or $g_B = 1/A$ when $A < 1$.

Figure 2 presents, for the case of $\phi = 0.64$ and $N = 16$ (recall this is the number of blocks of a single 4×4 square lattice used in the enclosure), the several configurations considered for each aspect ratio A. Included in the insets are details of two grids used in the computations. When the enclosure is shallow, $A \geq 1$, square lattices are placed horizontally side-by-side inside the enclosure. For A equal to 2, for instance, then $g_B = 2$ and $N_{tot} = 2N$. When the enclosure is tall, $A < 1$, the square lattices are placed vertically inside the enclosure; for instance, when $A = 0.25$ then $g_B = 4$, and $N_{tot} = 4N$.

Observe that when varying A, with N and ϕ constants, the distance from either isothermal wall up to the first column of blocks (shown as S_B in Figure 2) remains the same. Also, the size of the block, represented by the block side length D, is in principle a parameter of the problem as well. However, once the total number of blocks N_{tot} and the fluid volume fraction ϕ in a lattice are set, the D value is determined via the relation $D = [A(1 - \phi)/N_{tot}]^{1/2} = [A(1 - \phi)/(Ng_B]^{1/2}$. In this relation, $(1 - \phi)$ represents the solid volume fraction; keep in mind that the solid volume fraction of the lattice is identical to that of the entire enclosure.

Grid tests to determine the effect of grid distribution in the numerical results indicate that very good results are obtained when using 80×160 control volumes within each lattice. Some results are validated in Table 2 for clear (of solid blocks) enclosures [15, 17, 23]. A few streamline and isotherm distributions, for $Ra = 10^6$ with the corresponding Nu_{av} and Ψ_{max} values, are exhibited in Figure 3 for different aspect ratios as well. The Nu_{av} predictions compared very well with the predictions from the correlations available in Bejan [24]. Table 3 brings additional verification, comparing the present and published results for the

Table 1 Parametric ranges used for characterizing the natural convection process

	Range
A	0.25–4
Ra	10^5–10^8
N	1–36
K	0.1–100
ϕ	0.36–0.84

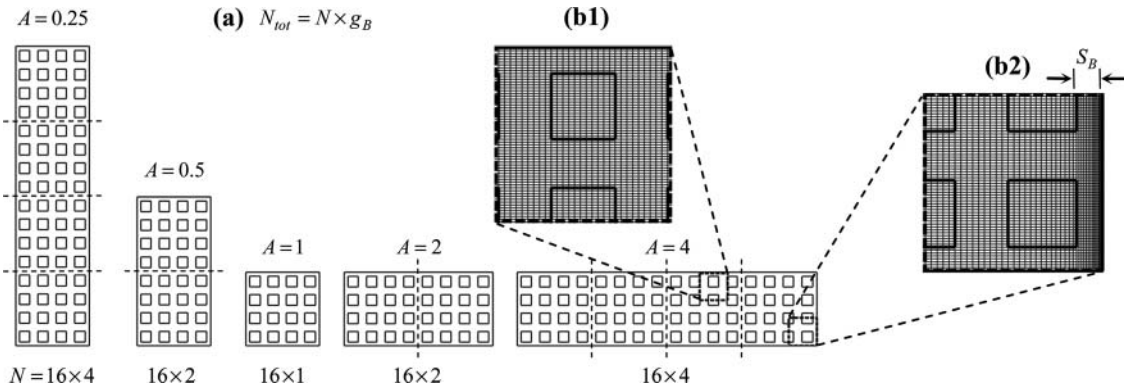

Figure 2 (a) Variation of total number of blocks, $N_{tot} = N \times g_B$, with A: number of lattices in the vertical direction is $g_B = 1/A$, for tall enclosures ($A < 1$), and in the horizontal direction is $g_B = A$, for shallow enclosures ($A \geq 1$). Insets show detail of uniform (b1) and of nonuniform computational grid (b2).

case of enclosures having a single, centered block. As can be seen, the present results compare very well.

Boundary-Layer Interference

One of the most significant influences of the solid blocks is the interference they can impose on the growth of the boundary layers that develop along the hot and cold surfaces of the enclosure. This interference is related to the distance between the column of blocks closest to the surface and the surface itself; considering the cold (right) surface, this distance in nondimensional form is labeled S_B in Figure 2(b2).

Considering the size of the blocks fixed for a moment, increasing the number of blocks inside the enclosure will reduce S_B. It is possible then to consider a situation in which S_B becomes too small for allowing the free development of the boundary layer along the hot and cold surfaces of the enclosure. When this happens, the blocks are said to "interfere" with the boundary layer, forcing the boundary layer to either be confined into a smaller channel or to bifurcate horizontally and around the

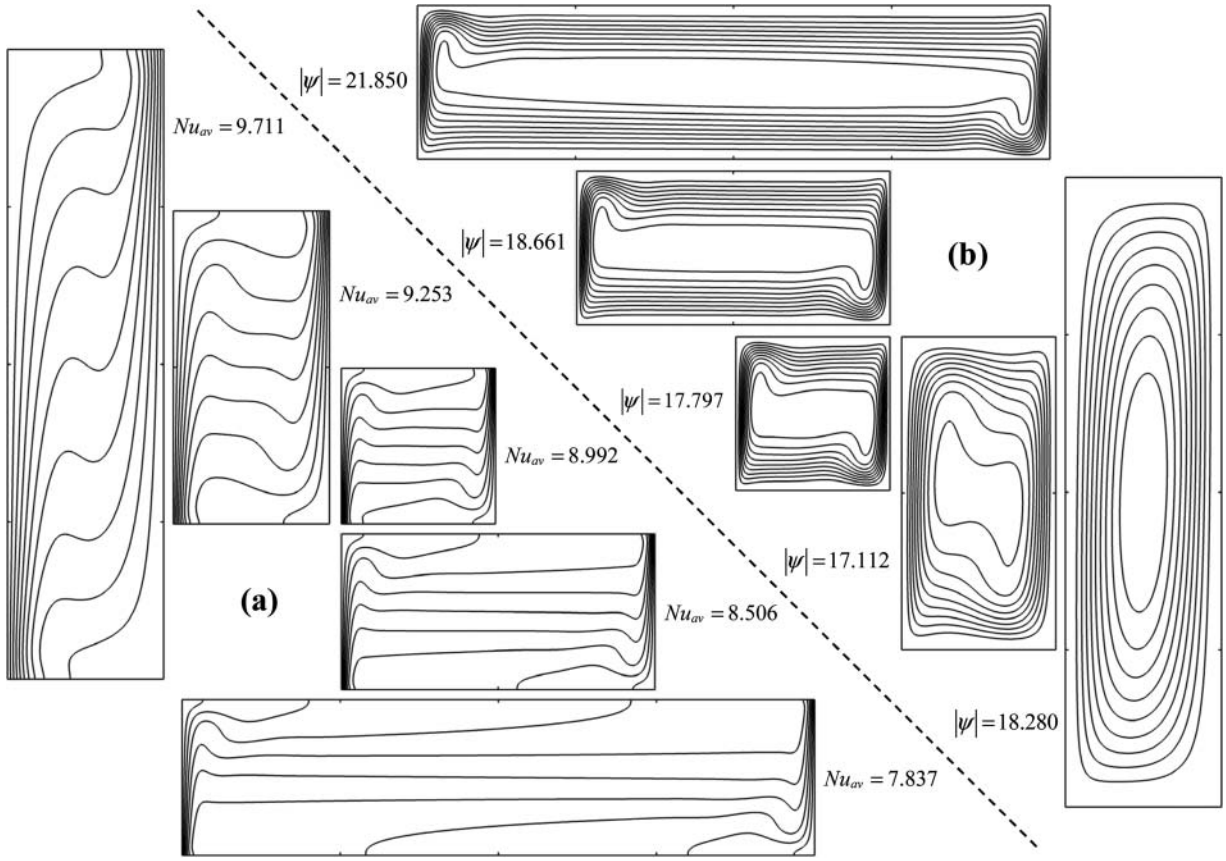

Figure 3 Effect on the natural convection process of varying $A = L/H$ for $Ra = 10^6$ in a clear (of solid blocks) fluid enclosure: (a) isotherms and (b) streamlines.

Table 2 Verification of numerical results based on Nu_{av} for the case of clear (of blocks) enclosure ($A = 1$)

Ra	Kalita et al. [23] $Pr = 0.71$	Merrikh and Lage [15] $Pr = 0.71$	Braga and de Lemos [17] $Pr = 1$	Present study $Pr = 1$
10^4	2.245	2.244	2.249	2.258
10^5	4.522	4.536	4.575	4.605
10^6	8.829	8.860	8.918	8.992
10^7	16.520	16.625	16.725	16.890
10^8	—	31.200	30.642	31.048

blocks. Therefore, as originally suggested by Merrikh and Lage [15], it is reasonable to assume the existence of a minimum number of blocks in the horizontal direction, N_{min}, beyond which the boundary layers along the hot and cold surfaces are affected in a pronounced way. Analogously to the concept of a N_{min}, a minimum porosity (ϕ_{min}) can be considered as well by recalling the relation between N, ϕ and D. Intuitively, a decrease in Ra would exacerbate the interference effect as consequence of the thicker boundary layer this change would induce.

The interference can be analytically predicted by setting the scale of the nondimensional boundary layer thickness for the natural convection, S_C, as greater than the nondimensional distance from the heated (or cooled) surface to the solid blocks, given by S_B. This comparison, obtained originally by Merrikh and Lage [15] for a square enclosure, has been recently extended to enclosures with any aspect ratio by Lage et al. [25], resulting in:

$$N_{min} = \left\{ \frac{A}{4Ra^{-1/4} g_B^*} - \frac{1}{4Ra^{-1/4}} \left[\frac{A}{g_B} (1 - \phi) \right]^{1/2} \right\}^2 \quad (13)$$

Notice that the function g_B^* in Eq. (13) is defined as equal to g_B if $A \geq 1$, or equal to unity otherwise.

A sample result from Eq. (13), in terms of N_{min} for achieving interference, is shown in Table 4, for $\phi = 0.64$ and various Ra and A values. Notice that the prediction of N_{min} becomes increasingly more sensitive to increases in Ra as A increases, and it becomes independent of A when $A \geq 1$ (shallow enclosures), as one would expect. Moreover, for $A = 0.25$ and $Ra = 10^5$ and 10^6, and for $A = 0.5$ and $Ra = 10^5$, the inclusion of a single block ($N_{min} = 1$) would yield block interference in the boundary layers. This indicates these tall enclosure configurations have the hot and cold surfaces close enough for the boundary layers to interfere with each other, even when the enclosure is clear of blocks.

Table 3 Verification of numerical results based on Nu_{av} for the case of a single block centered in the enclosure ($A = 1$, $Pr = 0.71$)

Ra	D	K	Bhave et al. [11]	Merrikh and Lage [15]	House et al. [5]	Present study
10^5	0.5	0.2	4.645	4.605	4.624	4.625
10^6	0.5	5.0	4.338	4.280	4.324	4.320
10^7	0.9	0.2	2.326	2.352	2.402	2.415
10^8	0.9	5.0	—	—	3.868	3.810

Table 4 Prediction of $N_{min} = f(Ra, A, \phi)$ for $\phi = 0.64$

	A				
Ra	0.25	0.5	1	2	4
10^5	1	1	4	4	4
10^6	1	4	16	16	16
10^7	4	9	36	36	36
10^8	9	25	100	100	100

Interestingly, this prediction is confirmed by the Nu_{av} numerical results displayed in Table 5. Observe that when $Ra = 10^5$ and $A = 0.25$, Nu_{av} quickly approaches the conductive regime when $N \geq 1$, for which case $Nu_{av} \sim (1/A)$. The same is true for when $Ra = 10^5$ and $A = 0.5$, and also when $Ra = 10^6$ and $A = 0.25$.

Table 4 shows also that the minimum number of blocks for interference grows very rapidly when $A \geq 1$ and $Ra \geq 10^6$, being greater than or equal to 16 blocks. Considering that the maximum number of blocks used here is 36, interference would not be observed in the extreme case of $N_{min} = 100$, predicted for when $Ra = 10^8$ and $A \geq 1$. Indeed, observe in the results of Table 5 for $Ra = 10^8$ that the abrupt variation in Nu_{av}, characteristic of when interference occurs, is not observable for any value of N.

Effect of Thermohydraulic Properties

The blocks also affect the thermal process inside the enclosure directly when conductive, as considered here, by offering a conduction path to the heat from the enclosure surface. This aspect is particularly important when there is interference, that

Table 5 Values of Nu_{av} for $\phi = 0.64$ and $K = 1$, for different A, N, and Ra

		A				
Ra	N	0.25	0.5	1	2	4
10^5	0	4.881	5.033	4.605	4.158	3.541
	1	4.042	3.171	4.328	3.385	2.050
	9	4.000	2.031	1.397	0.785	0.343
	16	4.000	2.016	1.244	0.675	0.299
	36	4.000	2.005	1.107	0.567	0.266
10^6	0	9.711	9.253	8.992	8.506	7.837
	1	6.181	8.900	8.932	8.354	7.328
	9	4.053	3.175	6.255	4.697	2.668
	16	4.027	2.783	4.347	3.102	1.641
	36	4.008	2.385	2.643	1.840	0.920
10^7	0	17.380	17.143	16.890	16.331	15.552
	1	16.682	17.102	16.728	16.246	15.438
	9	6.008	12.652	16.019	14.638	12.643
	16	5.352	8.546	15.208	13.832	11.553
	36	4.641	5.758	11.895	10.423	7.827
10^8	0	31.245	31.079	31.048	30.265	29.406
	1	31.514	30.920	30.940	30.145	29.297
	9	20.828	30.525	30.914	29.805	28.232
	16	14.235	28.918	30.488	29.098	27.364
	36	10.653	20.740	29.952	28.589	26.588

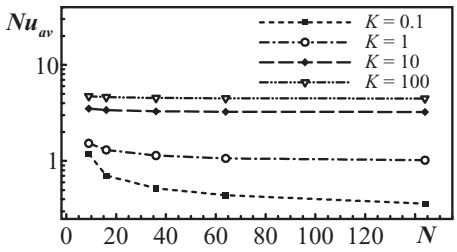

Figure 4 Effect of N on Nu_{av}, for $\phi = 0.36$, $Ra = 10^6$, $A = 1$, and several K values.

is, when the boundary layer arrives at the blocks before the end of the hot or cold surfaces. The thermohydraulic property that rules the conduction participation by the blocks is the solid–fluid thermal conductivity ratio (K). The studies of Merrikh and Mohamad [13] and Merrikh and Lage [15] considered the K effect; the former investigated the natural convection inside an enclosure with $A = 0.5$ and $N = 6$ and varying D, and the latter analyzed the effect of K on the heat transfer for a range of N maintaining the fluid volume-fraction constant ($\phi = 0.64$).

Figure 4 presents results of Nu_{av} versus N for $\phi = 0.36$, $Ra = 10^6$, and $A = 1$ and four different K values. Keep in mind that the analytical prediction for block interference, Eq. (13), for this case is $N_{min} = 4$ when $\phi = 0.36$.

In considering how K would affect Nu_{av}, if N is greater than or equal to N_{min} then the blocks are expected to interfere with the boundary layers. In this case, if K is greater than unity the blocks would help the heat transfer process by providing a less resistive path (higher thermal conductivity) along the horizontal direction than the path eventually provided by the fluid. Hence, one would expect K to mitigate the interference and possibly even lead to an increase in Nu_{av}. On the other hand, if K is less than unity, then one would expect a reduction in the Nu_{av} value. The results of Figure 4 seem to support these predictions. Observe how the Nu_{av} drops when N increases beyond N_{min} (equal to 4), for $K \leq 1$, with the effect being stronger for $K = 0.1$ than for $K = 1$. For cases when $K > 1$, however, the Nu_{av} seems not to be affected by varying N, as if the block interference effects were not present. Consider now the results of Nu_{av} versus N for $\phi = 0.84$, $Ra = 10^6$, and $A = 1$ and four different K values, shown in Figure 5. In this case, the analytical prediction for block interference, Eq. (13), is $N_{min} = 25$ when $\phi = 0.84$. The results show that varying K seem to have almost no effect on Nu_{av} when ϕ is large. With $N_{min} = 25$, not much interference is

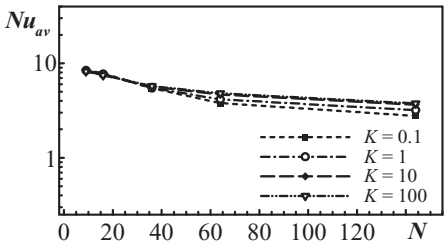

Figure 5 Effect of N on Nu_{av}, for $\phi = 0.84$, $Ra = 10^6$, $A = 1$, and several K values.

observed when N is small. Notice, however, the results show a small effect when varying K for $N \geq 25$.

Of course, one would expect the presence of the blocks to affect the flow inside the enclosure as well, by affecting the horizontal flows that develop along the top and bottom surfaces. This effect should be more pronounced when shallow enclosures are considered, that is, when A > 1, simply because these enclosures would offer a longer horizontal path to the fluid between the hot and cold surfaces. To investigate this aspect more closely, the setting $\phi = 0.64$, $K = 1$, and $Ra = 10^7$ is considered for $A = 2$ (shallow enclosure). Observe in this case, from Eq. (13), $N_{min} = 36$. Results for isotherm (a) and streamline (b) distributions for different N, in addition to Nu_{av} and Ψ, are shown in Figure 6.

Observe how the entrainment of the vertical boundary layers is visible only when $N = 36$, as predicted. This is confirmed by the abrupt drop of Nu_{av} value, from 13.8 for $N = 16$ to 10.4 for $N = 36$. What is interesting, and somewhat unexpected, is the reduction in Nu_{av} observed even before N reaches N_{min}. Notice, for instance, how Nu_{av} drops from 16.2 when $N = 2$, to 14.6 when $N = 9$, to 13.8 when $N = 16$. These decreases are not consequence of the interference effect in the vertical boundary

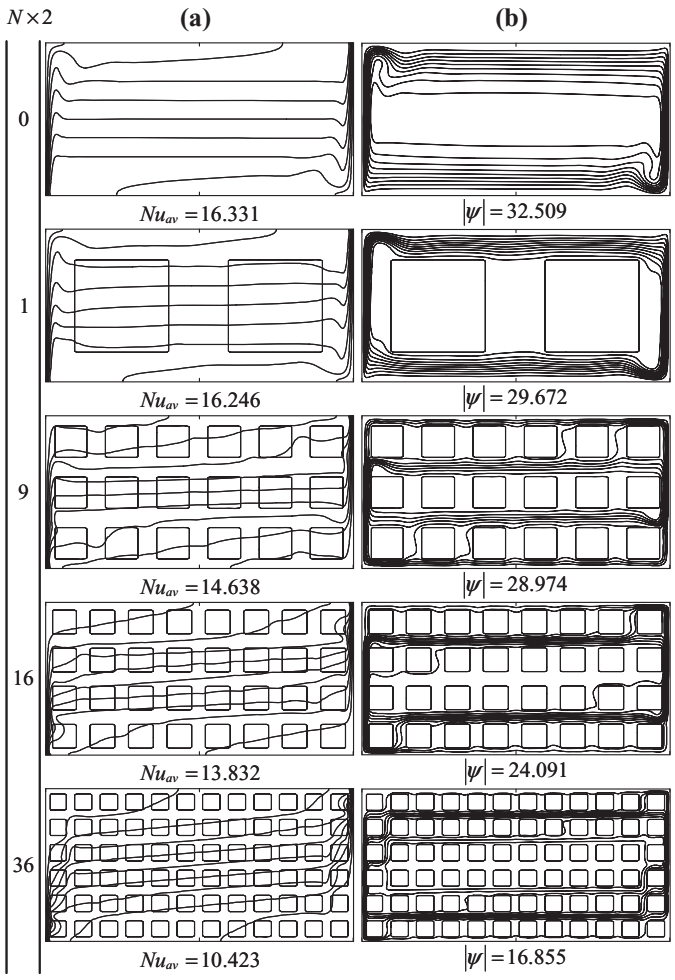

Figure 6 Effect of varying N on (a) isotherms and (b) streamlines for $A = 2$, $Ra = 10^7$, $\phi = 0.64$, and $K = 1$.

layer, but rather the result of the interference effect in the horizontal direction. Observe in the streamline plots how the fluid travels from left to right through the channels provided by the blocks away from the enclosure top surface (similarly, the fluid travels from right to left, away from the bottom surface). This natural "channeling" effect in the horizontal direction is the response of the flow to the stronger flow resistance imposed by the contiguous top and bottom surfaces of the enclosure. Although alleviating the pressure drop, the heat transfer is compromised when the boundary layer has had no chance to developed fully in the vertical direction (when $N < N_{min}$).

The effect of changing the number of blocks is considered in Figure 7, where Nu_{av} is plotted versus N for $\phi = 0.64$ and $K = 1$, and for several A and Ra values. The N_{min} values for each case can be obtained from Table 4. Clear from these graphs is that in all cases increasing N yields a smaller Nu_{av}. The effect of increasing N, however, varies depending on the aspect ratio of the enclosure A, and on Ra. When A is smaller than 1, the decrease in Nu_{av} as N increases happens more abruptly than when A is larger than 1, particularly when Ra is high. This reflects the aspect-ratio effect on N_{min}: As A increases toward 1, N_{min} increases as well, delaying the effect of increasing N past N_{min}. In other words, the system becomes less sensitive to the interference by the blocks when A and Ra are large. The reduction in Nu_{av} when A and Ra are large, as shown in the graphs, is likely due to an increase in the overall resistance of the flow due to the increase in N. This effect is expected to be more persistent when A is large, because of the longer trajectory the fluid has to flow to go from the heated surface to the cooled surface of the enclosure.

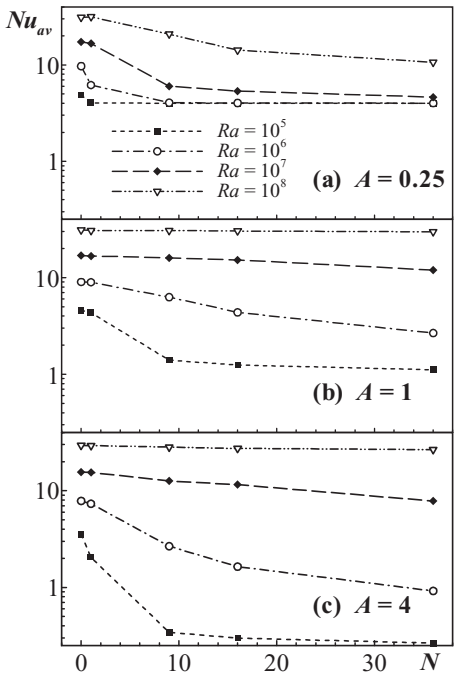

Figure 7 Variation of Nu_{av} versus N for several Ra, $\phi = 0.64$ and $K = 1$: (a) $A = 0.25$, (b) $A = 1$, and (c) $A = 4$.

A sample of the effect the aspect ratio has on the flow is presented in Figure 8, where the streamline and isotherm distributions are presented for $Ra = 10^6$, $N = 16$, $\phi = 0.64$, and $K = 1$. Keep in mind that when the aspect r atio departs from 1, either to a smaller value or a greater value, the total number of blocks in the enclosure increases (recall $N_{tot} = N \times g_B$). Interesting in the streamline plots is the persistence of flow away from the enclosure surfaces. Observe the predominant flow circulation in the first channel away from the vertical and horizontal enclosure surfaces. This aspect corroborates once more the N_{min} predictions provided by Eq. (13), which in this case is less than 16 for all A values considered. That is, for all aspect ratios, the number of blocks used is larger than the minimum necessary for the blocks to interfere with the boundary layers: All cases have interference! That is why the flow departs from the vertical surfaces in all configurations. The departure of the flow from the channel adjacent to the top and bottom horizontal surfaces is justified by the resistance provided by these channels, as explained before. Also interesting is that the flow intensity increases as A changes from 0.25 to 0.5 to 1, as seen by the Ψ values shown in the figure. Notice again that the configuration with $A = 0.25$ yields almost a pure diffusion heat transfer, as indicated by the isotherms being almost vertical, the Ψ value being very small, and $Nu_{av} \sim 1/A$. The convection strength increases for $A = 0.5$, and even more for $A = 1$, yielding corresponding larger values of Nu_{av}. The flow strength decreases as A increases further, leading to a decrease in Nu_{av}, simply because of the progressively longer extension separating the hot and cold surfaces.

SUMMARY AND CONCLUSIONS

The steady natural convection process in a heterogeneous, rectangular enclosure, filled with a saturating fluid and several disconnected solid square blocks resembling a geological formation, was studied. The effects of changing the volume fraction of the solid constituent, $(1 - \phi)$, the solid–fluid thermal conductivity ratio, K, and the total number of blocks inside the enclosure, N_{tot}, for several Rayleigh numbers Ra and enclosure aspect ratios A were presented in terms of the surface-averaged Nusselt number, Nu_{av}, and streamfunction Ψ, for a fluid with a fixed Prandtl number equal to unity.

The results, for $(1 - \phi)$ varying from 0.16 to 0.74, K from 0.1 to 100, N_{tot} from 0 to 144, Ra from 10^5 to 10^8, and A from 0.25 to 4, indicate the importance of block interference on the development of the boundary layers along the hot and cold surfaces of the enclosure. Using a previously proposed analytical expression for determining the minimum number of blocks, N_{min}, beyond which interference takes place, the somewhat erratic behavior of Nu_{av} can be explained and predicted.

Beginning with an enclosure without any blocks, the effect of increasing A is usually minor, and in the direction of reducing Nu_{av}. However, when solid blocks are present, the effect of increasing A becomes more pronounced, with Nu_{av} decreasing more abruptly the larger N is, when Ra is small. However,

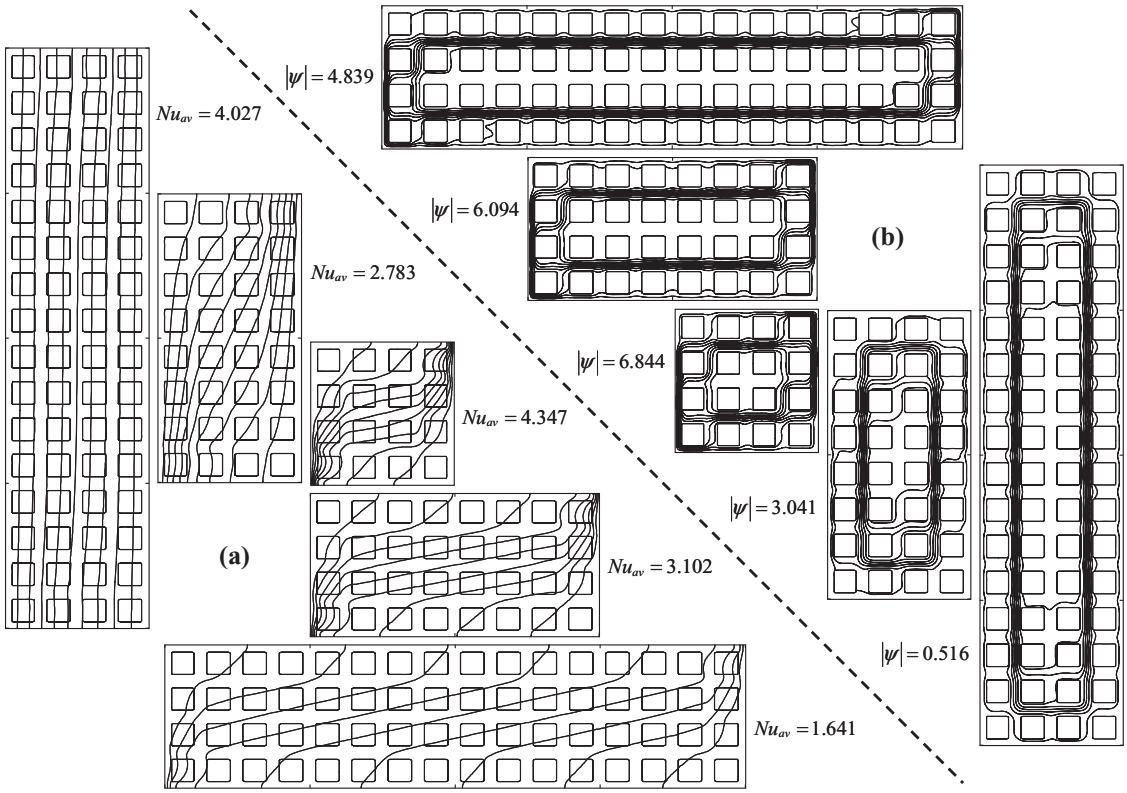

Figure 8 Effect on the natural convection of varying A for $Ra = 10^6$, $N = 16$, $\phi = 0.64$, and $K = 1$: (a) isotherms and (b) streamlines.

for high Ra the effect on Nu_{av} as A increases can invert, with Nu_{av} increasing substantially as A increases and then eventually decreasing. This anomalous behavior is explained by the interference of the solid blocks. Moreover, the effect of increasing ϕ is to increase Nu_{av}, with the increase being more dramatic for small N values as N_{min} increases with ϕ. Contrary to what might be expected, increasing K only leads to an appreciable increase in Nu_{av} when interference is present, in which case the blocks become active thermal participants in the natural convection process inside the enclosure. On the other hand, the effect of increasing N_{tot} is always to decrease Nu_{av}, with the decrease being more dramatic when N is less than N_{min}.

NOMENCLATURE

A	enclosure aspect ratio, $A = L/H$
c	specific heat, $J/kg \cdot K$
D	nondimensional length of the blocks
g	gravitational acceleration, m/s^2
g_B	number of lattices to fill enclosure
h	heat transfer coefficient, $W/m^2 \cdot K$
H	enclosure height, m
k	thermal conductivity, $W/m \cdot K$
K	solid–fluid thermal conductivity ratio
L	enclosure horizontal length, m
n	unit vector normal to the boundary
N	number of solid blocks within a lattice
N_{min}	minimum number of blocks for boundary layer interference
Nu	Nusselt number
p	dimensional pressure, Pa
P	nondimensional pressure
Pr	Prandtl number
Ra	Rayleigh number
S_B	nondimensional distance from the isothermal wall to the solid blocks
S_C	nondimensional boundary layer thickness
T	dimensional temperature, K
u, v	Cartesian velocity components along x and y directions, m/s
U, V	nondimensional Cartesian velocities
x, y	horizontal and vertical Cartesian coordinates, m
X, Y	non-dimensional Cartesian coordinates

Greek Symbols

α	thermal diffusivity, m^2/s
β	fluid isobaric coefficient of volumetric thermal expansion, $1/K$
ϕ	fluid volume fraction, porosity
ϕ_{min}	minimum porosity for boundary layer interference
μ	dynamic viscosity, $kg/m \cdot s$
ν	kinematic viscosity, m^2/s
θ	non-dimensional temperature

ρ density, kg/m^3
Ψ nondimensional streamfunction

Subscripts

av average
C cold
f fluid
H hot
i, j auxiliary index
min minimum
s solid
tot total

REFERENCES

[1] Nield, D. A., and Bejan, A., *Convection in Porous Media,* 2nd ed., Springer-Verlag, New York, NY, 1998

[2] Vafai, K., ed., *Handbook of Porous Media*, Marcel Dekker, New York, NY, 2000.

[3] Bejan, A., and Kraus, A. D., eds., *Heat Transfer Handbook*, Wiley, New York, NY, 2003.

[4] Merrikh, A. A., Lage, J. L., and Mohamad, A. A., Natural Convection in Non-Homogeneous Heat-Generating Media: Comparison of Continuum and Porous-Continuum Models, *Journal of Porous Media*, vol. 8, pp. 149–163, 2005.

[5] House, J. M., Beckermann, C., and Smith T. F., Effect of a Centered Conducting Body on Natural Convection Heat Transfer in an Enclosure, *Numerical Heat Transfer, Part A*, vol. 18, pp. 213–225, 1990.

[6] Oh, J. Y., Ha, M. Y., and Kim, K. C., Numerical Study of Heat Transfer and Flow of Natural Convection in an Enclosure With a Heat-Generating Conducting Body, *Numerical Heat Transfer, Part A*, vol. 31, pp. 289–303, 1997.

[7] Lee, J. R., and Ha, M. Y., A Numerical Study of Natural Convection in a Horizontal Enclosure with a Conducting Body, *International Journal of Heat and Mass Transfer*, vol. 48, pp. 3308–3318, 2005.

[8] Lee, J. R., and Ha, M. Y., Numerical Simulation of Natural Convection in a Horizontal Enclosure With a Heat-Generating Conducting Body, *International Journal of Heat and Mass Transfer*, vol. 49, pp. 2684–2702, 2006.

[9] Zhao, F. Y., Tang, G. F., and Liu, D., Conjugate Natural Convection in Enclosures With External and Internal Heat Sources, *International Journal of Engineering Science*, vol. 44, pp. 148–165, 2006.

[10] Zhao, F. Y., Liu, D., and Tang, G. F., Application Issues of the Streamline, Heatline and Massline for Conjugate Heat and Mass Transfer, *International Journal of Heat and Mass Transfer*, vol. 50, pp. 320–334, 2007.

[11] Bhave, P., Narasimhan, A., and Rees, D. A. S., Natural Convection Heat Transfer Enhancement Using Adiabatic Block: Optimal Block Size and Prandtl Number Effect, *International Journal of Heat and Mass Transfer*, vol. 49, pp. 3807–3818, 2006.

[12] Kumar De, A., and Dalal, A., A Numerical Study of Natural Convection Around a Square, Horizontal, Heated Cylinder Placed in an Enclosure, *International Journal of Heat and Mass Transfer*, vol. 49, pp. 4608–4623, 2006.

[13] Merrikh, A. A., and Mohamad, A. A., Blockage Effects in Natural Convection in Differentially Heated Enclosure, *Journal of Enhanced Heat Transfer*, vol. 8, pp. 55–74, 2001.

[14] Merrikh, A. A., and Lage, J. L., Effect of Distributing a Fixed Amount of Solid Constituent Inside a Porous Medium Enclosure on the Heat Transfer Process, *Proceedings of International Conference on Applications of Porous Media*, pp. 51–57, 2004.

[15] Merrikh, A. A., and Lage, J. L., Natural Convection in an Enclosure with Disconnected and Conducting Solid Blocks, *International Journal of Heat and Mass Transfer*, vol. 48, pp. 1361–1372, 2005.

[16] Hooman, K., and Merrikh, A. A., Theoretical Analysis of Natural Convection in an Enclosure Filled with Disconnected Conducting Square Solid Blocks, *Transport in Porous Media*, vol. 85, pp. 641–651, 2010.

[17] Braga, E. J., and de Lemos, M. J. S., Heat Transfer in Enclosures Having a Fixed Amount of Solid Material Simulated with Heterogeneous and Homogeneous Models, *International Journal of Heat and Mass Transfer*, vol. 48, pp. 4748–4765, 2005.

[18] Pourshaghaghy, A., Hakkaki-Fard, A., and Mahdavi-Nejad, A., Direct Simulation of Natural Convection in Square Porous Enclosure, *Energy Conversion and Management*, vol. 48, pp. 1579–1589, 2007.

[19] Massarotti, N., Nithiarasu, P., and Carotenuto, A., Microscopic and Macroscopic Approach for Natural Convection in Enclosures Filled With Fluid Saturated Porous Medium, *International Journal of Numerical Methods for Heat & Fluid Flow*, vol. 13, pp. 862–886, 2003.

[20] Braga, E. J., and de Lemos, M. J. S., Laminar Natural Convection in Cavities Filled With Circular and Square Rods, *International Communications in Heat and Mass Transfer*, vol. 32, pp. 1289–1297, 2005.

[21] Kimura, S., and Bejan, A., The 'Heatline' Visualization of Convective Heat Transfer, *ASME Journal Heat Transfer*, vol. 105, pp. 916–919, 1983.

[22] Patankar, S. V., and Spalding, D. B., A Calculation Procedure for Heat, Mass and Momentum Transfer in Three-Dimensional Parabolic Flows, *International Journal of Heat and Mass Transfer*, vol. 5, pp. 1787–1806, 1972.

[23] Kalita, J. C., Dalal, D. C., and Dass, A. K., Fully Compact Higher Order Computation of Steady-state Natural Convection in a Square Cavity, *Physical Review E*, vol. 64, pp. 1–13, 2001.

[24] Bejan, A., *Heat Transfer*, Wiley, New York, NY, 1993.

[25] Lage, J. L., De Lai, F. C., Junqueira, S. L. M., and Franco, A. T., Aspect-Ratio Effect on the Prediction of Boundary

Layer Interference in Natural Convection Inside Heterogeneous Enclosures, *International Journal of Heat and Mass Transfer*, 2013.

Silvio L. M. Junqueira received his Ph.D. in 1996 at the State University of Campinas, Brazil. He is currently an associate professor at the Federal Technological University–Paraná (UTFPR), Brazil. He works in thermal sciences, with emphasis on modeling and numerical simulation of transport phenomena in heterogeneous systems and the flow of drilling fluids in oil wells.

Fernando C. De Lai is a mechanical engineer associated with the Thermal Sciences Laboratory (LACIT) at the Federal Technological University–Paraná (UTFPR), Brazil. He received his B.Sc. degree in mechanical engineering in 2009, with a capstone project titled "Natural convection in a cavity filled with heterogeneous porous media." He is currently pursuing an M.Sc. in mechanical engineering. His research interests include the mathematical and computational modeling of transport phenomena in fractured porous media, with emphasis on micro- and macroscopic approaches at the pore or fracture scales.

Admilson T. Franco is an associate professor of mechanical engineering at Federal Technological University–Paraná, Brazil. He received his Ph.D. from State University of Campinas in 1999. He worked as a senior consulting in the cooling electronics field. His research interests include numerical simulation of heat transfer and fluid flow and non-Newtonian fluid mechanics. He has been investigating convection heat transfer in cavities and flow of viscoplastic fluids in well drilling.

José L. Lage is a professor of mechanical engineering at Southern Methodist University (SMU) and the director of the SMU Laboratory for Porous Materials Applications. His research has been supported by the NSF, NIST, DOE, and several industries. He is a fellow of the ASME, an honorary member of Pi Tau Sigma, a licensed professional engineer in the state of Texas, and the holder of a patent on "Cold Plate Design for Thermal Management of Phased-Array Radar Systems." He has received several awards, including an honorary professorship from the University "Dunarea de Jos" of Galati, Romania, the SAE Ralph R. Teetor Educational Award, the ASME-NTS Engineer of the Year Award, the ASEE Outstanding Teaching Award, the SMU Golden Mustang Award, and the Sigma Xi Outstanding Research Award.